

DO BARS TRIGGER ACTIVITY IN GALACTIC NUCLEI?

GWANG-HO LEE¹, JONG-HAK WOO¹, MYUNG GYOON LEE¹, HO SEONG HWANG^{2,3}, JONG CHUL LEE^{1,4}, JUBEE SOHN¹, AND
JONG HWAN LEE¹

¹Department of Physics and Astronomy, Seoul National University, 1 Gwanak-ro, Gwanak-gu, Seoul 151-742, Republic of Korea

²CEA Saclay/Service d'Astrophysique, F-91191 Gif-sur-Yvette, France

³Smithsonian Astrophysical Observatory, 60 Garden Street, Cambridge, MA 02138, USA and

⁴Korea Astronomy and Space Science Institute 776, Daedeokdae-ro, Yuseong-gu, Daejeon 305-348, Republic of Korea

Draft version November 26, 2018

ABSTRACT

We investigate the connection between the presence of bars and AGN activity, using a volume-limited sample of $\sim 9,000$ late-type galaxies with axis ratio $b/a > 0.6$ and $M_r < -19.5 + 5\log h$ at low redshift ($0.02 \leq z \lesssim 0.055$), selected from Sloan Digital Sky Survey Data Release 7. We find that the bar fraction in AGN-host galaxies (42.6%) is ~ 2.5 times higher than in non-AGN galaxies (15.6%), and that the AGN fraction is a factor of two higher in strong-barred galaxies (34.5%) than in non-barred galaxies (15.0%). However, these trends are simply caused by the fact that AGN-host galaxies are on average more massive and redder than non-AGN galaxies because the fraction of strong-barred galaxies (f_{SB}) increases with $u - r$ color and stellar velocity dispersion. When $u - r$ color and velocity dispersion (or stellar mass) are fixed, both the excess of f_{SB} in AGN-host galaxies and the enhanced AGN fraction in strong-barred galaxies disappears. Among AGN-host galaxies we find no strong difference of the Eddington ratio distributions between barred and non-barred systems. These results indicate that AGN activity is not dominated by the presence of bars, and that AGN power is not enhanced by bars. In conclusion we do not find a clear evidence that bars trigger AGN activity.

Subject headings: galaxies: active – galaxies: nuclei – galaxies: Seyfert – galaxies : spiral – galaxies : statistic

1. INTRODUCTION

Galactic bars are believed to play a crucial role in galaxy evolution. By reducing angular momentum, galactic bars can efficiently transport gas from outer disk to the central kiloparsec scale (Lynden-Bell 1979; Sellwood 1981; van Albada & Roberts 1981; Combes & Gerin 1985; Pfenniger & Friedli 1991; Heller & Shlosman 1994; Bournaud & Combes 2002; Athanassoula 2003; Jogee 2006), as demonstrated by a number of numerical simulations (e.g., Roberts et al. 1979; Athanassoula 1992; Friedli & Benz 1993; Maciejewski et al. 2002; Regan & Teuben 2004). The bar-driven gas can cause a mass accumulation within the Inner Lindblad Resonance (ILR), leading to the destruction of bars and the formation of pseudo-bulges (Hasan & Norman 1990; Pfenniger & Norman 1990; Hasan et al. 1993; Norman et al. 1996; Das et al. 2003; Shen & Sellwood 2004; Athanassoula et al. 2005; Bournaud et al. 2005). Numerous observational studies have found the characteristics of the bar-driven gas: i.e., inflow velocities from CO emission (e.g., Quillen et al. 1995; Benedict et al. 1996) and from H α emission (e.g., Regan et al. 1997), higher H α luminosities in barred galaxies than in non-barred galaxies (e.g., Ho et al. 1997), and higher molecular gas concentrations in the central kiloparsec region of barred galaxies (e.g.,

Sakamoto et al. 1999; Sheth et al. 2005).

Because of the high efficiency of gas inflow toward the central region of galaxies, bars are often invoked as a trigger of nuclear star formation. Enhanced nuclear star formation has been found in the central regions of barred spiral galaxies (e.g., Heckman 1980; Hawarden et al. 1986; Devereux 1987; Arsenault 1989; Huang et al. 1996; Ho et al. 1997; Martinet & Friedli 1997; Emsellem et al. 2001; Knapen et al. 2002; Jogee et al. 2005; Hunt et al. 2008; Bang & Ann 2009). Some statistical studies presented high bar fractions among star-forming galaxies: e.g., 61% in Ho et al. (1997), 82%-85% in Hunt & Malkan (1999), and 95% in Laurikainen et al. (2004).

Bar-driven gas inflow has been also considered as a mechanism for triggering active galactic nucleus (AGN) activity (Combes 2003). For the past three decades, much effort has been devoted to understand the connection between the presence of bars and AGN activity. However, it is not yet clear whether bars transport gas down to the vicinity of supermassive black holes (SMBHs). Several observational studies claimed that the fraction of barred galaxies is higher in AGN-host galaxies than in non-AGN galaxies (Arsenault 1989; Knapen et al. 2000; Laine et al. 2002), while many others found no significant excess of barred galaxies in AGN-host galaxies (Moles et al. 1995; McLeod & Rieke 1995; Mulchaey & Regan 1997; Ho et al. 1997; Laurikainen et al. 2004; Hao et al. 2009; Bang & Ann 2009).

Shlosman et al. (1989) suggested the “bars within bars” scenario as a mechanism for fueling AGNs. In this

ghlee@astro.snu.ac.kr
woo@astro.snu.ac.kr
mglee@astro.snu.ac.kr
hhwang@cfa.harvard.edu
jcleee@kasi.re.kr
jbsohn@astro.snu.ac.kr
leejh@astro.snu.ac.kr

model, large-scale stellar bars transport gas into their rotating disks of a few hundred parsec scale. When a critical amount of gas is accumulated, the disks undergo gravitational instability, triggering a gaseous secondary bar, which enables gas to approach closer to SMBHs (Mulchaey & Regan 1997; Maciejewski & Sparke 1997; Ho et al. 1997). Some studies suggested that nuclear spirals, instead of secondary bars, are responsible for triggering AGNs (Martini & Pogge 1999; Márquez et al. 2000; Martini et al. 2003). In a recent high-resolution smoothed particle hydrodynamics simulation, Hopkins & Quataert (2010) showed that disk instabilities (for 10 – 100 pc scales) driven by primary bars exhibit various morphologies as well as bar-like shapes. Several observational studies confirmed the presence of secondary bars by detecting nuclear bars embedded in large-scale bars, using the ISAAC/VLT spectroscopic data (Emsellem et al. 2001), the Hubble Space Telescope (HST) images (Malkan et al. 1998; Laine et al. 2002; Carollo et al. 2002; Erwin & Sparke 2002), and the integral field spectrograph SAURON data (Emsellem et al. 2006). It is found, however, that the fraction of secondary bars in AGNs is similar to that in non-AGNs (Martini et al. 2003), implying that secondary bars do not play a critical role in fueling AGNs. Although there have been many attempts, the nature of the AGN-bar connection is still unclear. The presence of secondary bars or nuclear spirals in non-AGN galaxies suggests that bars are not a universal fueling mechanism (Márquez et al. 2000; Laine et al. 2002; Martini et al. 2003).

In this paper, we investigate the connection between the presence of bars and AGN activity using a large sample of galaxies from the Sloan Digital Sky Survey (SDSS; York et al. 2000). SDSS data have been used by several previous studies in revealing the dependence of the bar fraction either on internal galaxy properties or on environmental properties (Barazza et al. 2008; Aguerri et al. 2009; Li et al. 2009; Nair & Abraham 2010b; Masters et al. 2011; Lee et al. 2012). However, the AGN-bar connection has not been studied in detail using the SDSS data. Hao et al. (2009) found no excess of bars in AGN-host galaxies using SDSS data. However, the galaxy sample in their study was relatively small and biased to blue galaxies (see Masters et al. 2011; Lee et al. 2012). Therefore, it is needed to investigate the connection between bars and AGN activity using a homogeneous and large galaxy sample. Following our detailed study on the relation between the presence of bars and galaxy properties (Lee et al. 2012, hereafter Paper I), we investigate the AGN-bar connection using a homogeneous sample of late-type galaxies, selected from the SDSS.

This paper is organized as follows. We describe the volume-limited sample and the method for identifying bars and spectral types in Section 2. Section 3 presents the main results including the dependence of the bar fraction on spectral types, the dependence of the AGN fraction on the presence of bars, and the comparison of Eddington ratio distributions between barred and non-barred AGN-host galaxies. We discuss the implication of primary results in Section 4, and present summary and conclusions in Section 5.

2. DATA AND METHODS

2.1. SDSS Galaxy Sample

We use a volume-limited sample of 33,391 galaxies with the r -band absolute magnitude $M_r \leq -19.5 + 5\log h$ mag (hereafter, we drop the $+5\log h$ term in the absolute magnitude) at redshift $0.02 \leq z \leq 0.05489$, from the SDSS Data Release 7 (DR7; Abazajian et al. 2009). These galaxies are extracted from the Korea Institute for Advanced Study Value-Added Galaxy Catalog (KIAS VAGC; Choi et al. 2010) that is based on the Large Scale Structure (LSS) sample of New York University Value-Added Galaxy Catalog (NYU VAGC; Blanton et al. 2005). The rest-frame absolute magnitudes of individual galaxies are computed in fixed bandpass, shifted to $z = 0.1$, using the Galactic reddening correction of Schlegel et al. (1998) and K -corrections as described by Blanton et al. (2003). The mean evolution correction given by Tegmark et al. (2004), $E(z) = 1.6(z - 0.1)$, is also applied. The spectroscopic parameters (i.e., stellar velocity dispersions and strength of various emission lines) are obtained from NYU VAGC and MPA/JHU DR7 VAGC (Tremonti et al. 2004; Brinchmann et al. 2004). Stellar masses are also from the MPA/JHU DR7 VAGC, which are based on fits to the SDSS five-band photometry (Kauffmann et al. 2003b). We adopt a flat Λ CDM cosmology with $\Omega_\Lambda = 0.74$ and $\Omega_m = 0.26$ from *Wilkinson Microwave Anisotropy Probe* five-year data (Komatsu et al. 2009).

The detailed description of the morphological classification and the identification of bars of the sample, and the comparison with previous classifications (de Vaucouleurs et al. 1991; Nair & Abraham 2010a) can be found in Paper I (see Section 3). We summarize the sample selection and classification schemes as follows. First, after dividing all galaxies into early- and late-type galaxies using the automated classification method (Park & Choi 2005) and visual inspection, we selected 19,431 late-type galaxies out of 33,391 galaxies (see Table 1 of Paper I). To avoid the internal extinction effects, we selected only galaxies with the minor-to-major axis ratio $b/a > 0.6$, obtaining a sample of 10,674 late-type galaxies. Then, we classified these late-type galaxies into three groups based on the presence (and the length) of bars: 2542 strong-barred (23.8%), 698 weak-barred (6.5%), and 7434 non-barred galaxies. When the size of bars is larger (shorter) than a quarter of the size of their host galaxies, we classified these galaxies as strong-barred (weak-barred) galaxies. As described in Paper I, our classification shows a good agreement with Nair & Abraham (2010a)’s classification.

In this study we classify the sample galaxies into AGNs and non-AGNs using the spectral features. To determine the spectral types and to investigate the dependence of the bar fraction on spectral types, we select galaxies whose spectra show strong emission-lines of $H\alpha$, $H\beta$, [OIII] $\lambda 5007$, and [NII] $\lambda 6584$ with signal-to-noise ratio $S/N \geq 3$ (Kewley et al. 2006). By excluding 2019 galaxies that do not satisfy the S/N criterion, we make a final the sample of 8655 late-type galaxies for the following analysis.

We perform the aperture correction to the velocity dispersion of the target galaxies using the equation sug-

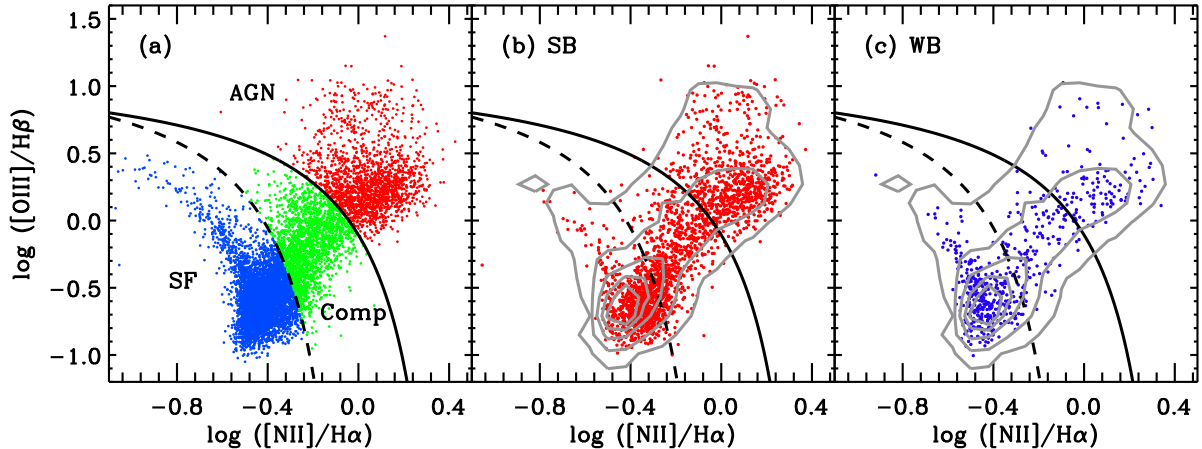


FIG. 1.— (a) Classification of spectral types for 8,655 late-type galaxies in the $[\text{NII}]/\text{H}\alpha$ versus $[\text{OIII}]/\text{H}\beta$ diagram. There are three types of galaxies (red: AGN-host galaxies, green: composite galaxies, and blue: star-forming galaxies) classified by two separate lines, the extreme starburst classification line (Kewley et al. 2001, solid line) and the pure star formation line (Kauffmann et al. 2003a, dashed line). In panels (b) and (c), dots represent strong-barred (SB) and weak-barred (WB) galaxies, respectively. Contours show the distribution for all late-type galaxies shown in panel (a).

TABLE 1
SPECTRAL TYPES OF THE SAMPLE GALAXIES

| Spectral type | $S/N^a \geq 3$ | | $S/N \geq 6$ | |
|---------------|----------------|----------|--------------|----------|
| | Number | Fraction | Number | Fraction |
| Star-forming | 4,940 | 57.1 % | 3,600 | 60.3 % |
| Composite | 1,973 | 22.8 % | 1,411 | 23.7 % |
| AGN-host | 1,742 | 20.1 % | 957 | 16.0 % |
| Total | 8,655 | 100 % | 5,968 | 100 % |

^a S/N for four emission lines such as $\text{H}\alpha$, $\text{H}\beta$, $[\text{NII}] \lambda 6584$, and $[\text{OIII}] \lambda 5007$

gested by Cappellari et al. (2006),

$$\sigma_{\text{corr}} = \sigma_{\text{fib}} \times (R_{\text{fib}}/R_{\text{eff}})^{(0.066 \pm 0.035)}, \quad (1)$$

where σ_{fib} is the velocity dispersion obtained from a fiber with $R_{\text{fib}} = 1''.5$. R_{eff} is an effective radius calculated by $R_{\text{eff}} = r_{\text{deV}} \times (b/a)_{\text{deV}}^{0.5}$ (Bernardi et al. 2003), where r_{deV} and $(b/a)_{\text{deV}}$ are, respectively, scale radius and b/a axis ratio in i -band in the de Vaucouleurs fit. Hereafter, the velocity dispersion means σ_{corr} , and its subscript corr will be omitted.

2.2. Classification of Spectral Types

To determine the spectral types, we use the $[\text{NII}]/\text{H}\alpha$ versus $[\text{OIII}]/\text{H}\beta$ diagnostic diagram that is known as Baldwin-Phillips-Terlevich (BPT) diagram (Baldwin et al. 1981; Veilleux & Osterbrock 1987). We categorize the sample galaxies into three spectral types: star-forming, composite, and AGN-host galaxies. As shown in Figure 1, Kewley et al. (2001) drew theoretical “maximum starburst lines” (solid lines) to define the upper boundary of star-forming galaxies, and Kauffmann et al. (2003a) added an empirical demarcation line (dashed line) to distinguish pure star-forming galaxies from composite galaxies whose spectra are affected by both star forming nuclei and AGNs.

We perform spectral classification using two criteria of S/N (for $\text{H}\alpha$, $\text{H}\beta$, $[\text{NII}]$, and $[\text{OIII}]$ emission lines): $S/N \geq 3$ and $S/N \geq 6$. When $S/N \geq 3$ is adopted, we find that the fractions of star-forming, composite, and AGN-host galaxies are 57.1% (4940 galaxies), 22.8%

(1973 galaxies), and 20.1% (1742 galaxies), respectively. On the other hand, in the case of $S/N \geq 6$, the sample galaxies consist of 60.3% (3600 galaxies) of star-forming, 23.7% (1411 galaxies) of composite, and 16.0% (957 galaxies) of AGN-host galaxies. The result of spectral classification is summarized in Table 1. As the threshold of S/N increases from 3 to 6, the fraction of AGN-host galaxies decreases 20.1% to 16.0%. This is because a significant fraction of LINERs in the low S/N sample is not included in the high S/N sample, since LINERs tend to dominate the low S/N sample (Cid Fernandes et al. 2010, 2011).

3. RESULTS

To investigate the connection between AGN activity and the presence of bars, first, we compare the bar fractions in AGN-host and non-AGN galaxies in Section 3.1. Then, we examine the AGN fraction between barred and non-barred galaxies in Section 3.2. Finally, using AGN host galaxies, we investigate whether the Eddington ratio distribution is different depending on the presence of bars in Section 3.3.

3.1. Dependence of Bar Fraction on AGN activity

Figure 1 shows the distributions of strong-barred (panel b) and weak-barred galaxies (panel c) in emission-line ratio diagrams ($[\text{NII}]/\text{H}\alpha$ versus $[\text{OIII}]/\text{H}\beta$). Strong-barred galaxies are widely distributed over the star-forming, composite, and AGN-host galaxy regions, while the majority of weak-barred galaxies lie in the star-forming galaxy region. Some weak bars are found in the composite and AGN-host galaxy region, but the number of those galaxies is relatively small.

We investigate how the bar fraction varies depending on the spectral types using two S/N criteria as summarized in Table 2. In the sample of 8655 galaxies with $S/N \geq 3$, the fraction of strong-barred galaxies (f_{SB}) is $15.6\% \pm 0.5\%$ in star-forming galaxies, $32.4\% \pm 1.1\%$ in composite galaxies, and $42.6\% \pm 1.1\%$ in AGN-host galaxies. Among 5968 galaxies with $S/N \geq 6$, f_{SB} is $18.3\% \pm 0.6\%$ in star-forming galaxies, $36.4\% \pm 1.3\%$ in composite galaxies, and $43.8\% \pm 1.6\%$ in AGN-host galax-

TABLE 2
DEPENDENCE OF BAR FRACTION ON SPECTRAL TYPES

| (1) $S/N^a \geq 3$ | | | | | | | |
|--------------------|-------|-----------------|---------------------------|-----------------|---------------|-------|-----------------|
| Spectral type | Total | SB ^b | f_{SB} (%) ^c | WB ^d | f_{WB} (%) | SB+WB | f_{SB+WB} (%) |
| Star-forming | 4,940 | 770 | 15.6 ± 0.5 | 348 | 7.0 ± 0.4 | 1,118 | 22.6 ± 0.6 |
| Composite | 1,973 | 639 | 32.4 ± 1.1 | 118 | 6.0 ± 0.5 | 757 | 38.4 ± 1.1 |
| AGN-host | 1,742 | 742 | 42.6 ± 1.1 | 109 | 6.3 ± 0.6 | 851 | 48.9 ± 1.2 |
| (2) $S/N \geq 6$ | | | | | | | |
| Spectral type | Total | SB | f_{SB} (%) | WB | f_{WB} (%) | SB+WB | f_{SB+WB} (%) |
| Star-forming | 3,600 | 659 | 18.3 ± 0.6 | 265 | 7.4 ± 0.4 | 924 | 25.7 ± 0.7 |
| Composite | 1,411 | 513 | 36.4 ± 1.3 | 67 | 4.7 ± 0.5 | 580 | 41.1 ± 1.3 |
| AGN-host | 957 | 419 | 43.8 ± 1.6 | 52 | 5.4 ± 0.7 | 471 | 49.2 ± 1.6 |

^a S/N for four emission lines such as $H\alpha$, $H\beta$, $[NII] \lambda 6584$, and $[OIII] \lambda 5007$

^b Strong-barred galaxies

^c The errors of the bar fraction are obtained by calculating the standard deviation in 1,000-times-repetitive sampling method.

^d Weak-barred galaxies

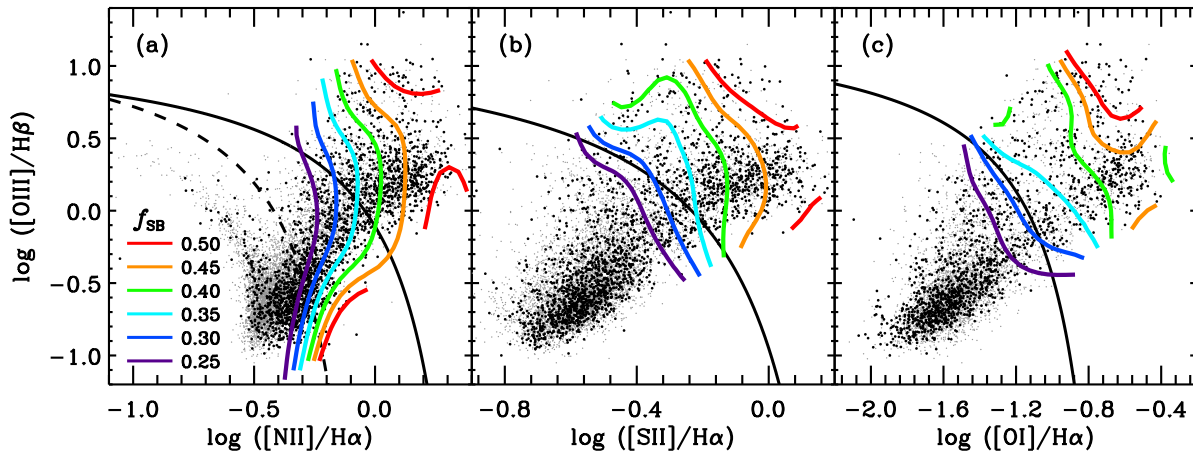


FIG. 2.— The fraction of strong-barred galaxies (f_{SB}) in the three BPT diagnostic diagrams: (a) $[NII]/H\alpha$ versus $[OIII]/H\beta$, (b) $[SII]/H\alpha$ versus $[OIII]/H\beta$, (c) $[OI]/H\alpha$ versus $[OIII]/H\beta$. Black dots and grey dots represent strong-barred galaxies and non-SB galaxies, respectively. Contours represent constant f_{SB} . In panels (b) and (c) we use only 8,508 galaxies with $S/N_{[SII]} \geq 3$ and 5,622 galaxies with $S/N_{[OI]} \geq 3$.

ies, respectively. In the low S/N case we find that f_{SB} is ~ 2.5 times higher in AGN-host galaxies than in star-forming galaxies. On the other hand, the fraction of weak-barred galaxies (f_{WB}) does not vary significantly with spectral types, from 6.0% to 7.0%. The result for the high S/N case is not different from that for the low S/N case.

Figure 2 presents the change of f_{SB} for the sample of galaxies with $S/N \geq 3$ in three BPT diagnostic diagrams such as (a) $[NII]/H\alpha$ versus $[OIII]/H\beta$, (b) $[SII]/H\alpha$ versus $[OIII]/H\beta$, and (c) $[OI]/H\alpha$ versus $[OIII]/H\beta$. In panel (b) we use 8508 galaxies with $S/N_{[SII]} \geq 3$, while only 5622 galaxies with $S/N_{[OI]} \geq 3$ are used in panel (c). We find a noticeable trend that f_{SB} increases continuously from the star-forming galaxy region (lower left) to the AGN-host galaxy region (upper right) in all diagnostic diagrams, showing that the presence of bars is more frequent in AGN-host galaxies than non-AGN galaxies. We check that this trend does not change significantly even when we use the high S/N sample.

In the view of the results we obtained above, it is seen that AGN activity is related to the presence of strong bars. However, we will see below that these results do

not directly indicate a connection between the presence of strong bars and AGN activity. This is because f_{SB} is also a strong function of galaxy properties, i.e., $u-r$ color, velocity dispersion (σ) and stellar mass (M_{star}). In Paper I, we found that $u-r$ and σ are more influential parameters in determining the bar fraction. Therefore, we need to compare AGN-host and non-AGN galaxies with fixed $u-r$ and σ in order to separate the effect of the two parameters on f_{SB} .

In Figure 3 we show the dependence of the bar fraction on three parameters: $u-r$, σ , and M_{star} . M_{star} is another important parameter affecting the bar fraction (e.g., Sheth et al. 2008; Cameron et al. 2010; Méndez-Abreu et al. 2010; Nair & Abraham 2010b). The fraction of strong-barred galaxies increases significantly as $u-r$ color becomes redder, and it has a maximum value at intermediate velocity dispersion of $\sim 130 \text{ km s}^{-1}$. It has a constant value ($\sim 10\%$) until $\log(M/M_{\odot}) = 10.2$, but increases with M_{star} thereafter. On the other hand, the fraction of weak-barred galaxies shows a different dependency on the three parameters. It has a peak value at a bluer color of $u-r \simeq 1.4$, and becomes larger as σ or M_{star} decreases. This result on M_{star} is consistent with the result of Nair & Abraham

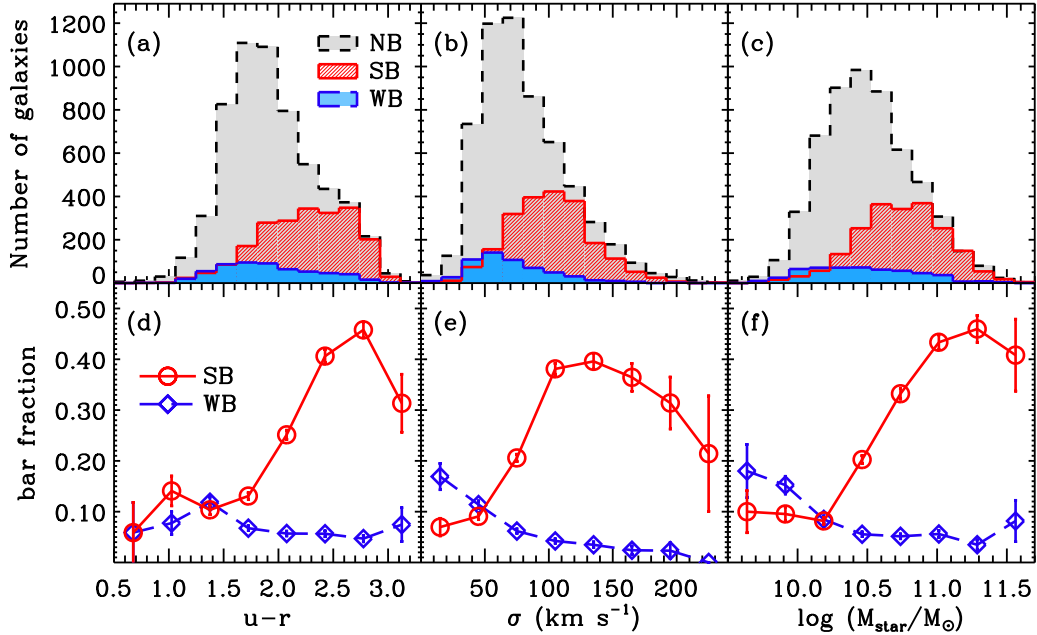


FIG. 3.— (Upper) The number of galaxies as a function of (a) $u-r$ color, (b) velocity dispersion (σ), and (c) stellar mass (M_{star}) for strong-barred (SB), weak-barred (WB), and non-barred (NB) galaxies. (Lower) The dependence of the bar fraction on (d) $u-r$, (e) σ , and (f) M_{star} . Circles and diamonds represent fractions of SB and WB galaxies, respectively. Error bars mean 1- σ sampling errors estimated by calculating the standard deviation of the bar fraction in 1,000-times-repetitive sampling.

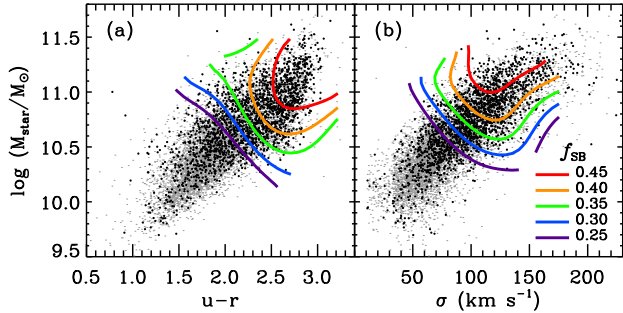


FIG. 4.— The fraction of strong-barred galaxies (f_{SB}) in (a) $u-r$ versus M_{star} diagram and (b) σ versus M_{star} diagram. Black dots and grey dots represent strong-barred galaxies and non-SB galaxies, respectively. Contours represent constant strong-barred galaxy fractions.

(2010b).

Figure 4 shows how f_{SB} varies in the $u-r$ versus M_{star} and in the σ versus M_{star} diagrams. It shows that M_{star} has a strong correlation with both $u-r$ and σ . It also shows that f_{SB} increases with the three parameters. However, at $\sigma \gtrsim 120$ km s⁻¹ it decreases with σ at a given M_{star} bin. Particularly, contours are neither vertical nor horizontal, suggesting that f_{SB} depends on the three parameters simultaneously. Therefore, we conclude that $u-r$, σ , and M_{star} are all important parameters in determining the bar fraction.

Because f_{SB} is strongly correlated with three parameters, we need to check whether the trend of f_{SB} in Figure 2 is originated from the effect of the three parameters on f_{SB} . To investigate the difference of $u-r$ and σ between AGN-host and non-AGN galaxies, we examine how $u-r$ and σ vary in the [NII]/H α versus [OIII]/H β diagnostic diagram as shown in Figure 5. We use 20×20 bins in this diagram to measure median values of $u-r$ and σ for late-type galaxies at each bin. After excluding bins that

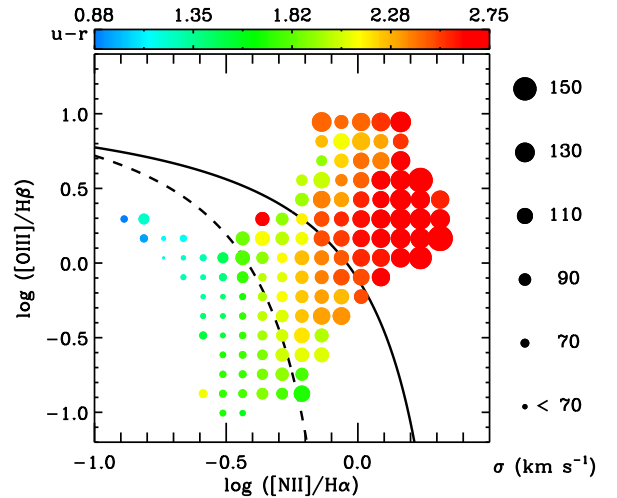


FIG. 5.— Distribution of $u-r$ and σ for 8,655 late-type galaxies in [NII]/H α versus [OIII]/H β diagnostic diagram. We divide this diagram into 20×20 bins and measure median values of $u-r$ and σ for galaxies at each bin. After excluding bins that contain less than five galaxies, we display representative symbols with various colors and sizes, corresponding to the median values of $u-r$ and σ , respectively.

contain less than five galaxies, we display representative symbols with various colors and sizes, corresponding to the median values of $u-r$ and σ , respectively. From the star-forming galaxy region toward the AGN-host galaxy region, it seems obvious that $u-r$ color becomes redder. At the same time, σ increases along the same direction. The median values of $u-r$ are 1.77 ± 0.01 , 2.20 ± 0.01 and 2.59 ± 0.01 , respectively for star-forming, composite, and AGN-host galaxies. In the case of σ , the median values for star-forming, composite, and AGN-host galaxies are 66.2 ± 0.5 , 95.1 ± 0.7 , and 118.3 ± 0.9 km s⁻¹, respectively. Considering the dependence of f_{SB} on $u-r$ and σ , it is

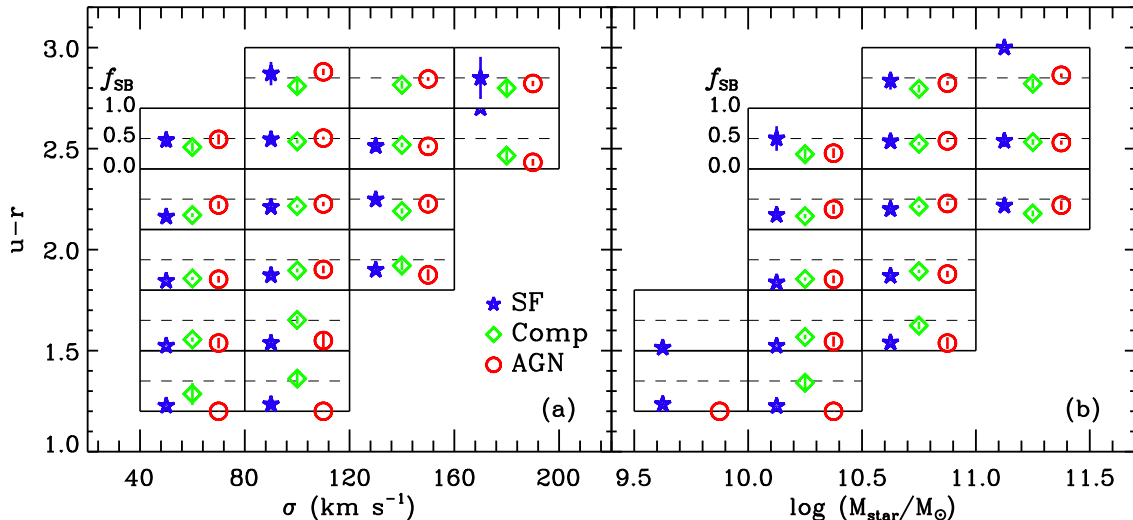


FIG. 6.— The dependence of the fraction of strong-barred galaxies (f_{SB}) on spectral types for late-type galaxies with fixed ranges of ($u-r$ ($\Delta(u-r) = 0.3$) and velocity dispersion ($\Delta\sigma = 40 \text{ km s}^{-1}$). (b) Same as (a), but x-axis is $\log(M_{\text{star}}/M_{\odot})$ instead of σ . Stars, diamonds, and circles with error bars represent f_{SB} for star-forming, composite, and AGN-host galaxies, respectively.

clear that the trend shown in Figure 2 is caused by the fact that f_{SB} increases with $u-r$ and σ (or M_{star}).

To remove the effect of $u-r$, σ , and M_{star} , we investigate the bar fraction in AGN-host and non-AGN galaxies at fixed $u-r$ and σ (or M_{star}), as shown in Figure 6. First, we divide our sample into 17 bins with fixed $u-r$ and σ ranges. Note that each bin contains more than fifty galaxies. Then we measure f_{SB} of each spectral type in each bin. An obvious excess of f_{SB} in AGN-host galaxies is found only in one bin with $u-r = 2.1 - 2.4$ and $\sigma = 40 - 80 \text{ km s}^{-1}$. In contrast, at all other $u-r$ and σ bins, f_{SB} of AGN-host galaxies is similar to that of star-forming galaxies. Second, we perform similar analysis at fixed $u-r$ and M_{star} ranges. We do not find any clear or significant excess of f_{SB} in AGN-host galaxies in all bins. These results clearly demonstrate that the f_{SB} excess in AGN-host galaxies shown in Figure 2 is caused by the fact that on average AGN-host galaxies are redder and more massive than non-AGN galaxies. These results suggest that the bar fraction do not depend on AGN activity.

3.2. Dependence of AGN Fraction on Bar Presence

In this section we investigate how AGN fraction changes depending on the presence of bars. Among non-barred or weak-barred galaxies, the fraction of star-forming galaxies ($> 60\%$) is much larger than that of AGN-host galaxies ($< 20\%$) while composite galaxies occupy $\sim 20\%$. In contrast, the AGN fraction increases by a factor of two when galaxies have strong bars. For example, among galaxies with $S/N \geq 3$ ($S/N \geq 6$), the AGN fraction is 34.5% (26.3%). AGN fractions in strong-barred, weak-barred, and non-barred galaxy samples are summarized in Table 3.

To demonstrate the dependence on galaxy properties, we present AGN fraction of barred (combining strong and weak bars) and non-barred galaxies, as a function of $u-r$, σ , and M_{star} in Figure 7. In both barred and non-barred galaxy samples, the AGN fraction increases with redder color, higher σ or larger M_{star} while the fraction of star-forming galaxies shows an opposite trend. At fixed

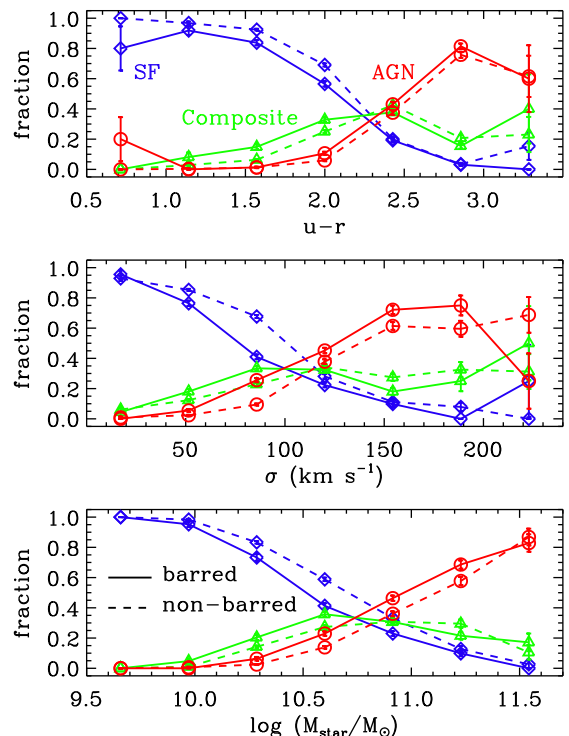


FIG. 7.— The fraction of AGN-host (circles), composite (triangles), and star-forming galaxies (diamonds) as a function of $u-r$ (top), σ (middle), and M_{star} (bottom). Solid lines and dashed lines represent barred (strong and weak-barred) and non-barred galaxies, respectively. Error bars mean 1- σ sampling errors.

σ or M_{star} , AGN fraction is significantly higher in barred galaxies than in non-barred galaxies. At fixed $u-r$ color, however, the excess of AGN fraction in barred galaxies is marginal. These results do not significantly change even if we exclude weak bars from the barred galaxy sample. The results presented in Figure 7 are similar to the finding of Oh et al. (2012, see their Figure 8), which appeared in the literature during the review process of our manuscript. We note that the sample size in this study is

TABLE 3
SPECTRAL CLASSIFICATION IN DIFFERENT BAR TYPES

| (1) $S/N^a \geq 3$ | | | | | | |
|--------------------|-----------------|----------|-----------------|----------|-----------------|----------|
| Spectral type | NB ^b | | SB ^c | | WB ^d | |
| | Number | Fraction | Number | Fraction | Number | Fraction |
| Star-forming | 3,822 | 64.5% | 770 | 35.8% | 348 | 60.5% |
| Composite | 1,216 | 20.5% | 639 | 29.7% | 118 | 20.5% |
| AGN-host | 891 | 15.0% | 742 | 34.5% | 109 | 19.0% |
| Total | 5,929 | 100.0% | 2,151 | 100.0% | 575 | 100.0% |

| (2) $S/N \geq 6$ | | | | | | |
|------------------|--------|----------|--------|----------|--------|----------|
| Spectral type | NB | | SB | | WB | |
| | Number | Fraction | Number | Fraction | Number | Fraction |
| Star-forming | 2,676 | 67.0% | 659 | 41.4% | 265 | 69.0% |
| Composite | 831 | 20.8% | 513 | 32.2% | 67 | 17.4% |
| AGN-host | 486 | 12.2% | 419 | 26.3% | 52 | 13.5% |
| Total | 3,993 | 100.0% | 1,591 | 100.0% | 384 | 100.0% |

^a S/N for four emission lines such as $H\alpha$, $H\beta$, $[NII] \lambda 6584$, and $[OIII] \lambda 5007$

^b Non-barred galaxies

^c Strong-barred galaxies

^d Weak-barred galaxies

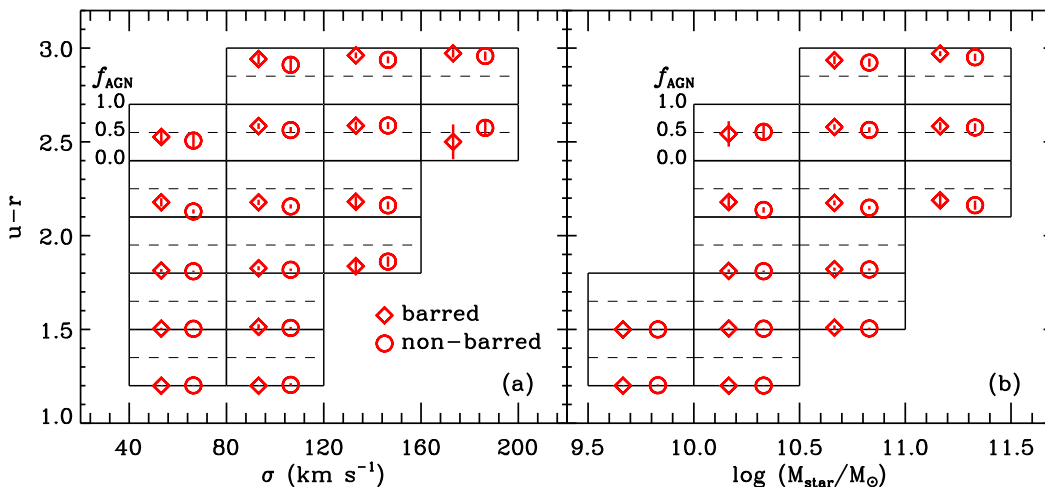


FIG. 8.— The dependence of the AGN fraction (f_{AGN}) on the presence of bars at fixed ranges of (a) $u-r$ and σ and (b) $u-r$ and M_{star} . Diamonds and circles represent f_{AGN} for barred (strong and weak-barred) and non-barred galaxies, respectively. Error bars represent 1- σ sampling errors.

much larger than that in Oh et al. (8655 galaxies versus 3934 galaxies), and that we classify composite galaxies separately instead of including them in the AGN sample.

The results in Figures 3, 4, and 7 show that both bar fraction and AGN fraction increase as galaxy color becomes redder. This leads naturally to an expectation that AGN and bars may be related. However, this does not necessarily mean that both are related. We need to investigate whether AGN is directly connected to bars or not.

For this we investigate whether AGN fraction is different between barred and non-barred galaxies in multi-dimensional spaces as shown in Figure 8. When we compare galaxies at fixed ranges of $u-r$ and σ (or M_{star}), the excess of AGN fraction in barred galaxies disappears or weakens. Within the sampling errors, there is no significant difference of AGN fraction between barred and non-barred galaxies. These results are dramatically different from those in Figure 7 due to the fact that AGN fraction is dependent of color and σ (or M_{star}). Figure 4

shows that $u-r$ has a large dispersion even when M_{star} is fixed. Similarly large color dispersion is also seen when σ is fixed (see Figure 9 in Paper I). Therefore an excess of the AGN fraction in barred galaxies shown in Figure 7 is an “apparent” trend, which is caused by the residual dependence on $u-r$ color in σ (or M_{star}) bins. Thus, in order to remove the effect of $u-r$ and σ (or M_{star}), AGN fraction has to be compared using galaxies at fixed $u-r$ AND σ (or M_{star}). We find no significant dependence of AGN fraction on the presence of bars, suggesting that AGN activity is not dominated by bars.

3.3. Comparison of Eddington Ratio between Barred and Non-barred AGN-host Galaxies

If AGN activity is triggered by bars, barred galaxies may have higher accretion rates than non-barred galaxies. We exclusively use AGN-host galaxies to examine whether there is any difference in AGN power between barred and non-barred galaxies.

We use the $[OIII]$ luminosity ($L_{[OIII]}$) as a proxy for the bolometric luminosity and infer black hole mass (M_{BH})

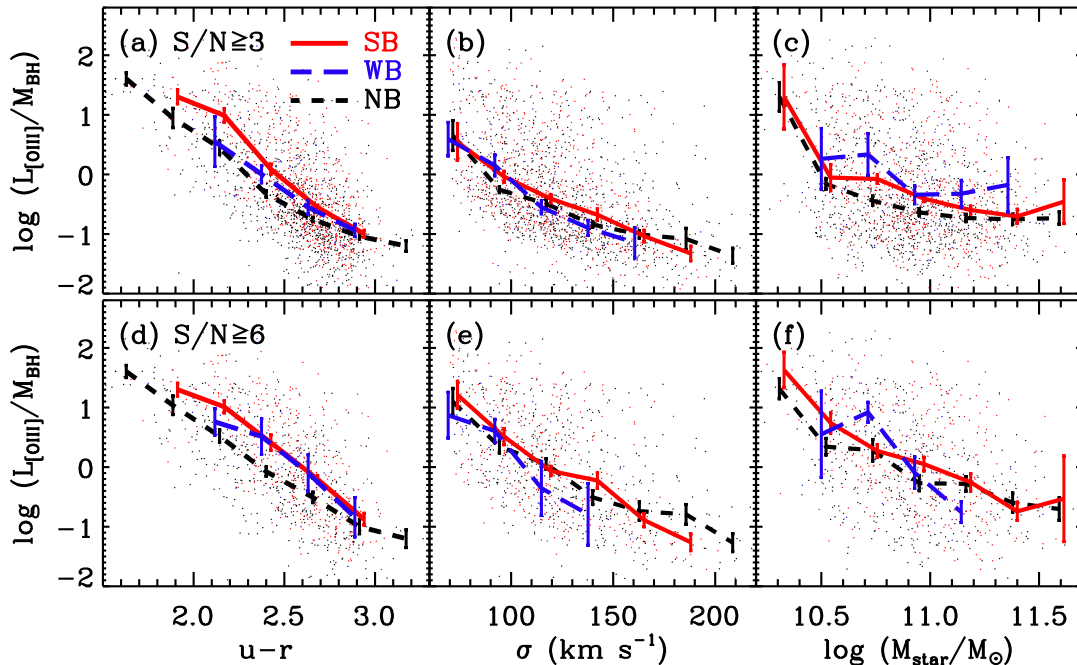


FIG. 9.— Eddington ratio as a function of (left) $u-r$, (middle) σ , and (right) M_{star} for 1,647 (upper, $S/N \geq 3$) and 893 (lower, $S/N \geq 6$) late-type AGN-host galaxies with $\sigma > 70 \text{ km s}^{-1}$. Solid lines, long-dashed lines, and short-dashed lines represent median curves of Eddington ratio for strong-barred (SB), weak-barred (WB), and non-barred (NB) AGN-host galaxies, respectively. The size of bins corresponds to $1/7$ of x-axis of each panel, and only when bins contain more than five galaxies median values of Eddington ratio are drawn. Error bars are calculated using 1,000-times resampling method. Error bars for strong-barred and weak-barred galaxies are slightly shifted respect to ones of non-barred galaxies in order to avoid overlap each other.

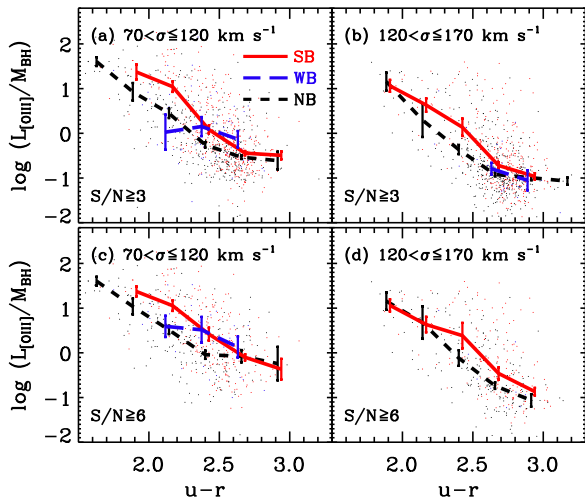


FIG. 10.— Eddington ratio versus $u-r$ for late-type AGN-host galaxies with (upper) $S/N \geq 3$, (lower) $S/N \geq 6$, (left) $70 \text{ km s}^{-1} < \sigma \leq 120 \text{ km s}^{-1}$, and (right) $120 \text{ km s}^{-1} < \sigma \leq 170 \text{ km s}^{-1}$. Solid lines, long-dashed lines, and short-dashed lines represent median curves of Eddington ratio for strong-barred (SB), weak-barred (WB), and non-barred (NB) galaxies, respectively. The size of bins corresponds to $1/7$ of x-axis of each panel, and only when bins contain more than five galaxies median values of Eddington ratio are drawn. Error bars are calculated using 1,000-times resampling method. Error bars for strong-barred and weak-barred galaxies are slightly shifted respect to ones of non-barred galaxies in order to avoid overlap each other.

from σ using Eq. (2) as described below. Thus, $L_{[\text{OIII}]}$ to M_{BH} ratio can be used as an approximate Eddington ratio indicator. We adopt a reddening curve of $R_V = A_V/E(B-V) = 3.1$ (Cardelli et al. 1989) and an intrinsic Balmer decrement of $\text{H}\alpha/\text{H}\beta = 3.1$ for AGN-

host galaxies (Osterbrock & Ferland 2006) to correct for internal dust extinction. To estimate M_{BH} , we adopt a $M_{\text{BH}} - \sigma$ relation for late-type galaxies suggested by McConnell et al. (2011):

$$\log(M_{\text{BH}}/M_{\odot}) = 7.97 + 4.58 \times \log(\sigma/200 \text{ km s}^{-1}). \quad (2)$$

We exclude galaxies with velocity dispersion values lower than the instrumental resolution of the SDSS spectra ($\sigma < 70 \text{ km s}^{-1}$) since these measurements are not reliable (Choi et al. 2009). In the following analysis we use two samples: 1647 AGN-host galaxies with $S/N \geq 3$ and 893 ones with $S/N \geq 6$. The low S/N sample contains 718 strong-barred, 97 weak-barred, and 832 non-barred galaxies. On the other hand, the high S/N sample consists of 407 strong-barred, 46 weak-barred, and 440 non-barred galaxies. The black hole mass of AGN-host galaxies spans $5.9 < \log(M_{\text{BH}}/M_{\odot}) < 8.3$, while $L_{[\text{OIII}]} / M_{\text{BH}}$ ranges over four order of magnitude, $10^{-2} - 10^2 L_{\odot} / M_{\odot}$.

In Figure 9 we present the Eddington ratio indicator (hereafter Eddington ratio) distributions as a function of $u-r$, σ , and M_{star} , respectively, for strong-barred, weak-barred, and non-barred galaxies. The AGN power (i.e., Eddington ratio) appears to decrease with M_{star} (or σ) as previously seen by Hwang et al. (2012). This trend can be interpreted as ‘‘Eddington incompleteness’’, which reflects the observational selection effect that for given flux (or luminosity limits) lower Eddington ratio AGNs can be detected at higher mass scales. Since at a fixed Eddington ratio it is harder to detect [OIII] lines for lower mass black holes, the Eddington ratios can be distributed down to a much lower values for higher mass black holes and galaxies as shown in Figure 9. In addition, we find that the AGN power is correlated with $u-r$ of galax-

ies. Blue AGN-host galaxies show significantly higher Eddington ratio than red AGN-host galaxies, implying that gas-rich systems generally have higher Eddington ratio than gas-poor systems. However, we note that this correlation can be also caused by the Eddington incompleteness since bluer color galaxies have on average lower galaxy (hence black hole) mass.

Nevertheless, we can compare the distributions of the Eddington ratio among strong-barred, weak-barred, and non-barred galaxies. We measure median values of $\log(L_{[\text{OIII}]} / M_{\text{BH}})$ as a function of $u - r$, σ , and M_{star} for each bar class. In panel (a) and (d), it is shown that median curves for strong-barred and weak-barred galaxies lie slightly above those for non-barred galaxies, although the differences between barred and non-barred galaxies are not significant and the median Eddington ratios are consistent within the error. In other panels there is no difference between barred and non-barred AGN-host galaxies over the whole ranges of σ and M_{star} .

To avoid the effect of Eddington incompleteness, we plot the Eddington ratio versus $u - r$ diagram at two fixed σ ranges in Figure 10. The anti-correlation between the Eddington ratio and $u - r$ is still present for both $70 \text{ km s}^{-1} < \sigma \leq 120 \text{ km s}^{-1}$ and $120 \text{ km s}^{-1} < \sigma \leq 170 \text{ km s}^{-1}$ ranges, indicating that AGN power is correlated with the amount of cold gas in galaxies. Choi et al. (2009) also found a similar result among late-type AGN-host galaxies with $7 < \log M_{\text{BH}} / M_{\odot} < 8$. We note that the contributions to the [OIII] lines from star formation can systematically increase the $L_{[\text{OIII}]} / M_{\text{BH}}$ ratio in bluer galaxies. Thus, further analysis is required to explore the connection between the presence of gas in large scales and the Eddington ratio.

When we compare the Eddington ratio distributions of barred and non-barred galaxies in Figure 10, the median values of the Eddington ratio are not significantly different, implying that AGN power is not strongly affected by the presence of bars. Considering the scatter in each bin, and the uncertainty and systematic errors in estimating black hole masses from the $M_{\text{BH}} - \sigma$ relation, we conclude that there is no strong difference of the Eddington ratios between barred and non-barred galaxies.

4. DISCUSSION

4.1. Do AGNs Favor Barred Galaxies?

Over the last three decades, bars have been invoked as a mechanism for fueling SMBHs. Although some studies claimed that AGNs are more frequently found in barred galaxies (Arsenault 1989; Knapen et al. 2000; Laine et al. 2002), no excess of bars in AGN-host galaxies has been reported by many other statistical studies (Moles et al. 1995; McLeod & Rieke 1995; Mulchaey & Regan 1997; Ho et al. 1997; Laurikainen et al. 2004; Hao et al. 2009). This discrepancy was at least in part caused by the small sample size, selection effect, and contamination owing to the correlation between bars and other galaxy properties, i.e., color and stellar mass.

In this study we find that the fraction of strong bars is ~ 2.5 times higher in AGN-host galaxies than in non-AGN galaxies. This result is clearly different from the findings by Hao et al. (2009), who claimed no excess of bar fraction in AGN-host galaxies based on a sample of

1,144 SDSS disk galaxies with $-18.5 > M_g > -22.0$ at $0.01 < z < 0.03$. The discrepancy is due to the combination of two effects. First, by using a color cut (Bell et al. 2004; Barazza et al. 2008) in selecting disk galaxies, Hao et al. (2009) inevitably excluded red disk galaxies, leading to a much lower AGN fraction in their sample (11.1%) than that in our sample (17.0%). Second, they used the ellipse fitting method to identify bars. In general the bar fraction based on the ellipse fitting (e.g., $\sim 50\%$ in r -band: Barazza et al. 2008) is much higher than that obtained by visual inspection (e.g., $\sim 33\%$ in B -band: de Vaucouleurs et al. 1991, $26\% \pm 0.5\%$ in $g+r+i$ color images: Nair & Abraham 2010a, $29.4\% \pm 0.5\%$ from Galaxy Zoo: Masters et al. 2010, Paper I, 36% : Oh et al. 2012). Thus, the combined effects of differences in sample selection and the classification method between Hao et al. and ours result in different findings.

We also find that the AGN fraction is twice higher in strong-barred galaxies than in non-barred galaxies as previous studies similarly reported (Arsenault 1989; Knapen et al. 2000; Laine et al. 2002). As shown in Figure 7, the higher AGN fraction in barred systems is present over a large ranges of M_{star} . This result is consistent with those of recent studies (Coelho & Gadotti 2011; Oh et al. 2012).

However, the excess of the bar fraction in AGN-host galaxies and the excess of the AGN fraction in barred galaxies do not indicate that the presence of bars and AGN activity are directly connected since the excess of the bar fraction in AGN-host galaxies and the excess of the AGN fraction in barred galaxies disappear when we compare galaxies with the same $u - r$ and σ (or M_{star}) (see Figure 6 and Figure 8). Thus, we conclude that AGN activity is not dominated by the presence of bars.

Comparing the Eddington ratios among AGN-host galaxies, we find no significant difference between barred and non-barred galaxies at fixed $u - r$, σ and M_{star} bins (see Figure 9), indicating that AGN power is not enhanced by the presence of bars.

Among AGN host galaxies with $2.0 < u - r < 2.5$, the Eddington ratios are marginally higher in strong-barred galaxies than in non-barred galaxies (see Figure 10), possibly implying that strong bars can boost AGN activity when their host galaxies lie in green valley. However, the number of AGN-host galaxies in our sample is not enough to draw a clear conclusion.

4.2. Dependence on the $M_{\text{BH}} - \sigma$ Relation

Since we estimate black hole masses from stellar velocity dispersion utilizing the $M_{\text{BH}} - \sigma$ relation, the derived Eddington ratios depend on the slope and intercept of the $M_{\text{BH}} - \sigma$ relation. Thus, it is necessary to investigate whether the Eddington ratio difference between barred and non-barred galaxies depends on the adopted $M_{\text{BH}} - \sigma$ relation.

Over the last decade, empirical scaling relations between M_{BH} and σ have been improved as the number of galaxies with M_{BH} measurements increased (e.g., Ferrarese & Merritt 2000; Gebhardt et al. 2000; Tremaine et al. 2002; Gültekin et al. 2009b; Graham & Li 2009; Woo et al. 2010). By combining two new M_{BH} measurements with the literature data published before August 2011, a recent study by McConnell et al. (2011) provided two $M_{\text{BH}} - \sigma$ rela-

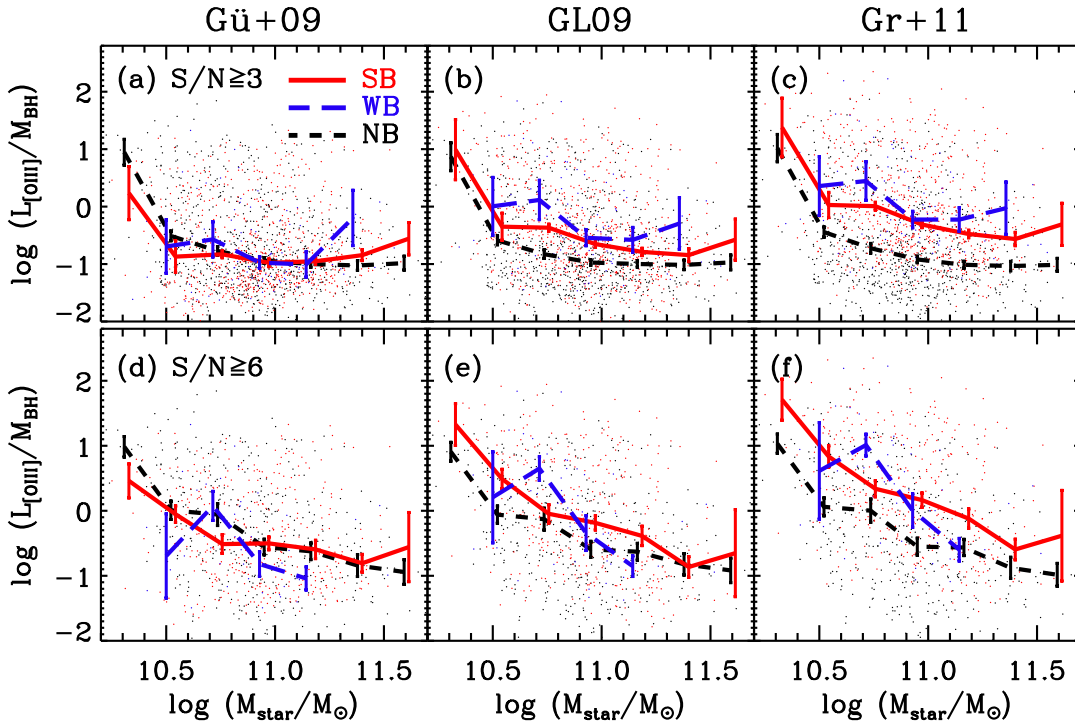


FIG. 11.— Comparison of Eddington ratio as a function of M_{star} between strong-barred (SB), weak-barred (WB), and non-barred (NB) AGN-host galaxies with (upper) $S/N \geq 3$, (lower) $S/N \geq 6$, when adopting $M_{\text{BH}} - \sigma$ relations given by (left) Gültekin et al. (2009b): $(\alpha, \beta) = (7.67, 1.08)$ for barred and $(8.19, 4.21)$ for non-barred, (middle) Graham & Li (2009): $(8.03, 3.94)$ for barred and $(8.15, 3.89)$ for non-barred, and (right) Graham et al. (2011): $(7.80, 4.34)$ for barred and $(8.25, 4.57)$ for non-barred galaxies, respectively.

tions; $\log(M_{\text{BH}}/M_{\odot}) = \alpha + \beta \log(\sigma/200\text{km s}^{-1})$ with $(\alpha, \beta) = (8.38 \pm 0.06, 4.53 \pm 0.40)$ for elliptical/S0 galaxies and $(7.97 \pm 0.22, 4.58 \pm 1.25)$ for spiral galaxies. In this study we adopt the second equation for estimating M_{BH} since our sample is composed of late-type galaxies.

A few studies separately derived $M_{\text{BH}} - \sigma$ relations for barred and non-barred galaxies (Gültekin et al. 2009b; Graham & Li 2009; Graham et al. 2011). For example, Gültekin et al. (2009b) reported $(\alpha, \beta) = (8.19 \pm 0.087, 4.21 \pm 0.446)$ for non-barred and $(7.67 \pm 0.115, 1.08 \pm 0.751)$ for barred galaxies while Graham & Li (2009) derived $(8.15 \pm 0.05, 3.89 \pm 0.18)$ for non-barred galaxies, and $(8.03 \pm 0.05, 3.94 \pm 0.19)$ for the combined sample of barred and non-barred galaxies. Graham et al. (2011) reported steeper $M_{\text{BH}} - \sigma$ relations with $(8.25 \pm 0.06, 4.57 \pm 0.35)$ for non-barred galaxies and $(7.80 \pm 0.10, 4.34 \pm 0.56)$ for barred galaxies.

To demonstrate the dependence of Eddington ratios on the adopted $M_{\text{BH}} - \sigma$ relation, we compare in Figure 11 Eddington ratios between barred and non-barred galaxies using three different pairs of $M_{\text{BH}} - \sigma$ relations mentioned above. When the $M_{\text{BH}} - \sigma$ relations from Gültekin et al. (2009b) are used, barred and non-barred galaxies show no significant difference in Eddington ratios as similarly shown in Figure 9. In contrast, Eddington ratios tend to be higher in barred galaxies than in non-barred galaxies when the $M_{\text{BH}} - \sigma$ relations are taken from Graham & Li (2009). The enhanced Eddington ratios in barred galaxies is particularly noticeable when using Graham et al. (2011)'s $M_{\text{BH}} - \sigma$ relations, since M in barred galaxies are significantly reduced due to the lower intercept of the $M_{\text{BH}} - \sigma$ relation.

If we adopt different $M_{\text{BH}} - \sigma$ relations respectively for

barred and non-barred galaxies, AGN power appears to be enhanced by bars. Oh et al. (2012) used the $M_{\text{BH}} - \sigma$ relations taken from Graham & Li (2009), and they argued that AGN strength is enhanced by the presence bars. However, there are several limitations in adopting two different relations for barred and non-barred. First, the $M_{\text{BH}} - \sigma$ relation of barred galaxies is not well defined since the relation has been derived with a small number of barred galaxies. For example, Gültekin et al. (2009b) used only 8 measurements (and 11 upper limits of M_{BH}) of barred galaxies while Graham et al. (2011) also used only 20 barred galaxies. Second, the $M_{\text{BH}} - \sigma$ relation of non-barred galaxies are biased to early-type galaxies since early-type galaxies are dominant in the sample. Third, dynamical mass measurements of black holes in barred galaxies are much more uncertain since no stellar dynamical model truly accounts for stellar bars (Gültekin et al. 2009a). Therefore, we decide to use only one $M_{\text{BH}} - \sigma$ relation for late-type galaxies as given in McConnell et al. (2011), in order to avoid any systematic uncertainties of the $M_{\text{BH}} - \sigma$ relations between barred and non-barred galaxies. It is necessary to investigate whether barred galaxies have higher Eddington ratios than non-barred galaxies when more robust $M_{\text{BH}} - \sigma$ relations of barred and non-barred late-type galaxies become available in the future.

4.3. What Triggers AGNs?

Based on the statistical analysis using a large sample of ~ 9000 late-type galaxies, we find that AGN activity is not dominated by the presence of bars. Then, what triggers AGNs?

Several numerical simulations suggested that interac-

tions and mergers between galaxies are main triggers for AGN activity (Noguchi 1987; Hernquist 1989; Barnes & Hernquist 1992, 1991; Mihos & Hernquist 1996; Di Matteo et al. 2005; Hopkins et al. 2006; Debuhr et al. 2011). This scenario is supported by several observational studies. For example, Sanders et al. (1988) showed that ultra-luminous infrared galaxies (ULIRG) and quasars are formed through the strong interaction or merger between gas-rich spirals. Bahcall et al. (1997) found that twenty nearby luminous quasars ($z < 0.3$) in their sample have galaxy companions that are closer than 25 kpc. In the case of lower luminosity AGNs, i.e., Seyfert galaxies, minor mergers between gas rich galaxies and with their satellite galaxies are proposed as a mechanism for triggering AGN activity (e.g., De Robertis et al. 1998). However, some observational studies showed conflicting results. Fuentes-Williams & Stocke (1988) found a marginal evidence that Seyfert galaxies interact with their companions that have comparable sizes. In addition, by investigating the environmental dependence of AGN fraction using the SDSS sample, Miller et al. (2003) claimed that the fraction of AGN-host galaxies is independent on environment (see also, Coziol et al. 1998; Shimada et al. 2000; Schmitt 2001).

Recently, Martínez et al. (2010) reported that AGN-host galaxies (45%) are more frequent than composite (23%) or star-forming galaxies (32%) in the Hickson compact group environment where galaxy-galaxy interactions occur violently. Hwang et al. (2012) and Choi et al. (in prep.) also found, using the SDSS data, that the AGN fraction increases as the distance to a nearest late-type neighbor galaxy decreases in both cluster and field environments, and concluded that AGN activity can be triggered through mergers and interactions between galaxies when gas supply for AGN is available. In contrast, da Silva et al. (2011) claimed that merging galaxies with signatures of recent starburst, found in the green valley, had no detectable AGN activity. Although it is theoretically clear that mergers and interactions between galaxies can provide advantages for AGN activity by reducing angular momentum of interstellar medium and by generating gas inflows to the center of galaxies, observational studies do not clearly show the connection between galaxy interaction and AGN activity.

Additional mechanisms are expected to occur at subkiloparsec scales in order to influence the central black hole directly. Secondary bars residing in the nuclear region, which are often called as nested bars, nuclear bars or inner bars, have been a strong candidate. Some observational works (Shaw et al. 1995; Wozniak et al. 1995; Friedli et al. 1996; Mulchaey & Regan 1997; Jungwiert et al. 1997; Greusard et al. 2000; Emsellem et al. 2001, 2006; Laurikainen et al. 2007) found secondary bars in the central region of galaxies. These secondary bars are predicted by the “bars within bars” scenario (Shlosman et al. 1989). The dynamical and kinematical properties of secondary bars are investigated by simulations (Englmaier & Shlosman 2004; Maciejewski & Athanassoula 2008; Shen & Debattista 2009, 2011) and by observations (Garcia-Burillo et al. 1998; Schinnerer et al. 2006; de Lorenzo-Cáceres et al. 2008). Similarly, nuclear dust spirals are invoked as

a means to transport material from kiloparsec scales down to sub-kpc scales. High resolution images from HST provided a close look at dusty structures in nuclear regions (Malkan et al. 1998; Regan & Mulchaey 1999; Martini & Pogge 1999; Pogge & Martini 2002). Martini et al. (2003) classified nuclear spirals into several morphological types: grand-design, tightly wound, loosely wound, chaotic nuclear spirals. Recently, Hopkins & Quataert (2010) showed that gas structures formed by gravitational instabilities at several parsec scale have diverse morphologies: spirals, rings, clumps and also bars. So, they proposed “stuff within stuff” model that is a revised version of Shlosman et al. (1989)’s model. However, there is another argument that the presence of nuclear spirals is not also directly connected with current AGN activity, because the frequency of nuclear spirals in AGN-host galaxies is comparable with that in non-AGN galaxies (Martini et al. 2003). Thus, further studies are needed to investigate any relation between nuclear spirals (or secondary bars) and activity in galactic nuclei.

5. SUMMARY AND CONCLUSIONS

We investigate the relation between the presence of bars and AGN activity, using a sample of 8655 late-type galaxies with $b/a > 0.6$ and $M_r < -19.5$ at $0.02 \leq z \leq 0.05489$, selected from the SDSS DR7. We divide these galaxies into three spectral types: star-forming, composite, and AGN-host galaxies, and classified them into barred (strong & weak) and non-barred galaxies by visual inspection. We summarize our main findings as follows.

1. The strong bar fraction is ~ 2.5 times higher in AGN-host galaxies than in star-forming galaxies. However, the excess of f_{SB} is caused by the fact that AGN-host galaxies have on average redder $u - r$ color and higher σ than non-AGN galaxies since f_{SB} is higher for redder and more massive (higher σ) galaxies. The excess of f_{SB} in AGN-host galaxies disappears when galaxies with the same $u - r$ and σ (or M_{star}) are compared, indicating that f_{SB} do not depend on AGN activity.

2. Strong-barred galaxies have higher AGN fraction than weak-barred or non-barred galaxies. However, we find no difference of the AGN fraction between barred and non-barred galaxies, when we compare galaxies with the same $u - r$ color and σ (or M_{star}), indicating that AGN activity is not dominated by the presence of bars.

3. Among AGN-host galaxies, barred and non-barred systems show similar Eddington ratio distributions as a function of $u - r$, σ , and M_{star} , implying that AGN power is not enhanced by bars.

In conclusion we do not find any evidence that bars trigger AGN activity. Thus we argue that there is no direct connection between AGN activity and the presence of bars.

We thank the anonymous referee for his/her useful comments which improved significantly the original manuscript. G.H.L. thank Changbom Park and Yun-Young Choi for providing help in producing the KIAS VAGC and performing the morphology classification. M.G.L. was supported in part by Mid-career Re-

search Program through the NRF grant funded by the MEST (no.2010-0013875). J.H.W. acknowledges support by the Basic Science Research Program through the

NRF funded by the MEST (no.2010-0021558). H.S.H. acknowledges the Centre National d'Etudes Spatiales (CNES) and the Smithsonian Institution for the support of his post-doctoral fellowship.

REFERENCES

- Abazajian, K. N., et al. 2009, *ApJS*, 182, 543
Aguerri, J. A. L., Méndez-Abreu, J., & Corsini, E. M. 2009, *A&A*, 495, 491
Arsenault, R. 1989, *A&A*, 217, 66
Athanasoula, E. 1992, *MNRAS*, 259, 345
Athanasoula, E. 2003, *MNRAS*, 341, 1179
Athanasoula, E., Lambert, J. C., & Dehnen, W. 2005, *MNRAS*, 363, 496
Bahcall, J. N., Kirhakos, S., Saxe, D. H., & Schneider, D. P. 1997, *ApJ*, 479, 642
Baldwin, J. A., Phillips, M. M., & Terlevich, R. 1981, *PASP*, 93, 5
Bang, J., & Ann, H. B. 2009, *The Journal of the Korean Earth Science Society*, 30, 1
Barazza, F. D., Jogee, S., & Marinova, I. 2008, *ApJ*, 675, 1194
Barnes, J. E., & Hernquist, L. 1992, *ARA&A*, 30, 705
Barnes, J. E., & Hernquist, L. E. 1991, *ApJ*, 370, L65
Bell, E. F., et al. 2004, *ApJ*, 608, 752
Benedict, F. G., Smith, B. J., & Kenney, J. D. P. 1996, *AJ*, 111, 1861
Bernardi, M., et al. 2003, *AJ*, 125, 1817
Blanton, M. R., et al. 2003, *AJ*, 125, 2348
Blanton, M. R., et al. 2005, *AJ*, 129, 2562
Bournaud, F., & Combes, F. 2002, *A&A*, 392, 83
Bournaud, F., Combes, F., & Semelin, B. 2005, *MNRAS*, 364, L18
Brinchmann, J., Charlot, S., White, S. D. M., et al. 2004, *MNRAS*, 351, 1151
Cameron, E., Carollo, C. M., Oesch, P., et al. 2010, *MNRAS*, 409, 346
Cappellari, M., et al. 2006, *MNRAS*, 366, 1126
Cardelli, J. A., Clayton, G. C., & Mathis, J. S. 1989, *ApJ*, 345, 245
Carollo, C. M., Stiavelli, M., Seigar, M., de Zeeuw, P. T., & Dejonghe, H. 2002, *AJ*, 123, 159
Choi, Y.-Y., Han, D.-H., & Kim, S. S. 2010, *Journal of Korean Astronomical Society*, 43, 191
Choi, Y.-Y., Woo, J.-H., & Park, C. 2009, *ApJ*, 699, 1679
Cid Fernandes, R., Stasińska, G., Schlickmann, M. S., et al. 2010, *MNRAS*, 403, 1036
Cid Fernandes, R., Stasińska, G., Mateus, A., & Vale Asari, N. 2011, *MNRAS*, 413, 1687
Coelho, P., & Gadotti, D. A. 2011, *ApJ*, 743, L13
Combes, F. 2003, *Active Galactic Nuclei: From Central Engine to Host Galaxy*, 290, 411
Combes, F., & Gerin, M. 1985, *A&A*, 150, 327
Coziol, R., de Carvalho, R. R., Capelato, H. V., & Ribeiro, A. L. B. 1998, *ApJ*, 506, 545
da Silva, R. L., Prochaska, J. X., Rosario, D., Tumlinson, J., & Tripp, T. M. 2011, *ApJ*, 735, 54
Das, M., Teuben, P. J., Vogel, S. N., Regan, M. W., Sheth, K., Harris, A. L., & Jefferys, W. H. 2003, *ApJ*, 582, 190
de Lorenzo-Cáceres, A., Falcón-Barroso, J., Vazdekis, A., & Martínez-Valpuesta, I. 2008, *ApJ*, 684, L83
De Robertis, M. M., Yee, H. K. C., & Hayhoe, K. 1998, *ApJ*, 496, 93
de Vaucouleurs, G., de Vaucouleurs, A., Corwin, H. G., Jr., Buta, R. J., Paturel, G., & Fouqué, P. 1991, *Third Reference Catalog of Bright Galaxies* (Berlin: Springer)
Debuhr, J., Quataert, E., & Ma, C.-P. 2011, *MNRAS*, 412, 1341
Devereux, N. 1987, *ApJ*, 323, 91
Di Matteo, T., Springel, V., & Hernquist, L. 2005, *Nature*, 433, 604
Emsellem, E., Greusard, D., Combes, F., Friedli, D., Leon, S., Pécontal, E., & Wozniak, H. 2001, *A&A*, 368, 52
Emsellem, E., Fathi, K., Wozniak, H., Ferruit, P., Mundell, C. G., & Schinnerer, E. 2006, *MNRAS*, 365, 367
Englmaier, P., & Shlosman, I. 2004, *ApJ*, 617, L115
Erwin, P., & Sparke, L. S. 2002, *AJ*, 124, 65
Ferrarese, L., & Merritt, D. 2000, *ApJ*, 539, L9
Friedli, D., & Benz, W. 1993, *A&A*, 268, 65
Friedli, D., Wozniak, H., Rieke, M., Martinet, L., & Bratschi, P. 1996, *A&AS*, 118, 461
Fuentes-Williams, T., & Stocke, J. T. 1988, *AJ*, 96, 1235
Gültekin, K., Richstone, D. O., Gebhardt, K., et al. 2009a, *ApJ*, 695, 1577
Gültekin, K., Richstone, D. O., Gebhardt, K., et al. 2009b, *ApJ*, 698, 198
García-Burillo, S., Sempere, M. J., Combes, F., & Neri, R. 1998, *A&A*, 333, 864
Gebhardt, K., Bender, R., Bower, G., et al. 2000, *ApJ*, 539, L13
Graham, A. W., Onken, C. A., Athanasoula, E., & Combes, F. 2011, *MNRAS*, 412, 2211
Graham, A. W., & Li, I.-h. 2009, *ApJ*, 698, 812
Greusard, D., Friedli, D., Wozniak, H., Martinet, L., & Martin, P. 2000, *A&AS*, 145, 425
Hao, L., Jogee, S., Barazza, F. D., Marinova, I., & Shen, J. 2009, *Galaxy Evolution: Emerging Insights and Future Challenges*, 419, 402
Hasan, H., & Norman, C. 1990, *ApJ*, 361, 69
Hasan, H., Pfenninger, D., & Norman, C. 1993, *ApJ*, 409, 91
Hawarden, T. G., Mountain, C. M., Leggett, S. K., & Puxley, P. J. 1986, *MNRAS*, 221, 41P
Heckman, T. M. 1980, *A&A*, 88, 365
Heller, C. H., & Shlosman, I. 1994, *ApJ*, 424, 84
Hernquist, L. 1989, *Nature*, 340, 687
Ho, L. C., Filippenko, A. V., & Sargent, W. L. W. 1997, *ApJ*, 487, 591
Hopkins, P. F., Hernquist, L., Cox, T. J., Di Matteo, T., Robertson, B., & Springel, V. 2006, *ApJS*, 163, 1
Hopkins, P. F., & Quataert, E. 2010, *MNRAS*, 407, 1529
Huang, J. H., Gu, Q. S., Su, H. J., Hawarden, T. G., Liao, X. H., & Wu, G. X. 1996, *A&A*, 313, 13
Hunt, L. K., et al. 2008, *A&A*, 482, 133
Hunt, L. K., & Malkan, M. A. 1999, *ApJ*, 516, 660
Hwang, H. S., Park, C., Elbaz, D., & Choi, Y.-Y. 2012, *A&A*, 538, A15
Jogee, S. 2006, *Physics of Active Galactic Nuclei at all Scales*, 693, 143
Jogee, S., Scoville, N., & Kenney, J. D. P. 2005, *ApJ*, 630, 837
Jungwiert, B., Combes, F., & Axon, D. J. 1997, *A&AS*, 125, 479
Kauffmann, G., et al. 2003a, *MNRAS*, 346, 1055
Kauffmann, G., Heckman, T. M., White, S. D. M., et al. 2003b, *MNRAS*, 341, 33
Kewley, L. J., Dopita, M. A., Sutherland, R. S., Heisler, C. A., & Trevena, J. 2001, *ApJ*, 556, 121
Kewley, L. J., Groves, B., Kauffmann, G., & Heckman, T. 2006, *MNRAS*, 372, 961
Knapen, J. H., Shlosman, I., & Peletier, R. F. 2000, *ApJ*, 529, 93
Knapen, J. H., Pérez-Ramírez, D., & Laine, S. 2002, *MNRAS*, 337, 808
Komatsu, E., et al. 2009, *ApJS*, 180, 330
Laine, S., Shlosman, I., Knapen, J. H., & Peletier, R. F. 2002, *ApJ*, 567, 97
Laurikainen, E., Salo, H., & Buta, R. 2004, *ApJ*, 607, 103
Laurikainen, E., Salo, H., Buta, R., & Knapen, J. H. 2007, *MNRAS*, 381, 401
Lee, G.-H., Park, C., Lee, M. G., & Choi, Y.-Y. 2012, *ApJ*, 745, 125 (Paper I)
Li, C., Gadotti, D. A., Mao, S., & Kauffmann, G. 2009, *MNRAS*, 397, 726
Lynden-Bell, D. 1979, *MNRAS*, 187, 101
Márquez, I., et al. 2000, *A&A*, 360, 431
Méndez-Abreu, J., Sánchez-Janssen, R., & Aguerri, J. A. L. 2010, *ApJ*, 711, L61
Maciejewski, W., & Athanasoula, E. 2008, *MNRAS*, 389, 545
Maciejewski, W., & Sparke, L. S. 1997, *ApJ*, 484, L117
Maciejewski, W., Teuben, P. J., Sparke, L. S., & Stone, J. M. 2002, *MNRAS*, 329, 502
Malkan, M. A., Gorjian, V., & Tam, R. 1998, *ApJS*, 117, 25
Martínez, M. A., Del Olmo, A., Coziol, R., & Perea, J. 2010, *AJ*, 139, 1199
Martinet, L., & Friedli, D. 1997, *A&A*, 323, 363
Martini, P., & Pogge, R. W. 1999, *AJ*, 118, 2646
Martini, P., Regan, M. W., Mulchaey, J. S., & Pogge, R. W. 2003, *ApJ*, 589, 774
Masters, K. L., et al. 2010, *MNRAS*, 405, 783
Masters, K. L., et al. 2011, *MNRAS*, 411, 2026
McConnell, N. J., Ma, C.-P., Gebhardt, K., et al. 2011, *Nature*, 480, 215
McLeod, K. K., & Rieke, G. H. 1995, *ApJ*, 441, 96
Mihos, J. C., & Hernquist, L. 1996, *ApJ*, 464, 641
Miller, C. J., Nichol, R. C., Gómez, P. L., Hopkins, A. M., & Bernardi, M. 2003, *ApJ*, 597, 142
Moles, M., Márquez, I., & Pérez, E. 1995, *ApJ*, 438, 604
Mulchaey, J. S., & Regan, M. W. 1997, *ApJ*, 482, L135
Nair, P. B., & Abraham, R. G. 2010a, *ApJS*, 186, 427
Nair, P. B., & Abraham, R. G. 2010b, *ApJ*, 714, L260
Noguchi, M. 1987, *MNRAS*, 228, 635
Norman, C. A., Sellwood, J. A., & Hasan, H. 1996, *ApJ*, 462, 114

- Oh, S., Oh, K., & Yi, S. K. 2011, *ApJS*, 198, 4
- Osterbrock, D. E. & Ferland, G. J. 2006, *Astrophysics of gaseous nebulae and active galactic nuclei*, 2nd edn. University Science Books, Mill Valley, CA
- Park, C., & Choi, Y.-Y. 2005, *ApJ*, 635, L29
- Pfenniger, D., & Friedli, D. 1991, *A&A*, 252, 75
- Pfenniger, D., & Norman, C. 1990, *ApJ*, 363, 391
- Pogge, R. W., & Martini, P. 2002, *ApJ*, 569, 624
- Quillen, A. C., Frogel, J. A., Kenney, J. D. P., Pogge, R. W., & Depoy, D. L. 1995, *ApJ*, 441, 549
- Regan, M. W., & Mulchaey, J. S. 1999, *AJ*, 117, 2676
- Regan, M. W., & Teuben, P. J. 2004, *ApJ*, 600, 595
- Regan, M. W., Vogel, S. N., & Teuben, P. J. 1997, *ApJ*, 482, L143
- Roberts, W. W., Jr., Huntley, J. M., & van Albada, G. D. 1979, *ApJ*, 233, 67
- Sakamoto, K., Okumura, S. K., Ishizuki, S., & Scoville, N. Z. 1999, *ApJ*, 525, 691
- Sanders, D. B., Soifer, B. T., Elias, J. H., Madore, B. F., Matthews, K., Neugebauer, G., & Scoville, N. Z. 1988, *ApJ*, 325, 74
- Schinnerer, E., Böker, T., Emsellem, E., & Lisenfeld, U. 2006, *ApJ*, 649, 181
- Schlegel, D. J., Finkbeiner, D. P., & Davis, M. 1998, *ApJ*, 500, 525
- Schmitt, H. R. 2001, *AJ*, 122, 2243
- Sellwood, J. A. 1981, *A&A*, 99, 362
- Shaw, M., Axon, D., Probst, R., & Gatley, I. 1995, *MNRAS*, 274, 369
- Shen, J., & Debattista, V. P. 2011, *Memorie della Societa Astronomica Italiana Supplementi*, 18, 169
- Shen, J., & Debattista, V. P. 2009, *ApJ*, 690, 758
- Shen, J., & Sellwood, J. A. 2004, *ApJ*, 604, 614
- Sheth, K., Elmegreen, D. M., Elmegreen, B. G., et al. 2008, *ApJ*, 675, 1141
- Sheth, K., Vogel, S. N., Regan, M. W., Thornley, M. D., & Teuben, P. J. 2005, *ApJ*, 632, 217
- Shimada, M., Ohyama, Y., Nishiura, S., Murayama, T., & Taniguchi, Y. 2000, *AJ*, 119, 2664
- Shlosman, I., Frank, J., & Begelman, M. C. 1989, *Nature*, 338, 45
- Tegmark, M., et al. 2004, *ApJ*, 606, 702
- Tremaine, S., Gebhardt, K., Bender, R., et al. 2002, *ApJ*, 574, 740
- Tremonti, C. A., et al. 2004, *ApJ*, 613, 898
- van Albada, G. D., & Roberts, W. W., Jr. 1981, *ApJ*, 246, 740
- Veilleux, S., & Osterbrock, D. E. 1987, *ApJS*, 63, 295
- Woo, J.-H., Treu, T., Barth, A. J., et al. 2010, *ApJ*, 716, 269
- Wozniak, H., Friedli, D., Martinet, L., Martin, P., & Bratschi, P. 1995, *A&AS*, 111, 115
- York, D. G., et al. 2000, *AJ*, 120, 1579